2021 43rd Annual International Conference of the
IEEE Engineering in Medicine & Biology Society (EMBC)
Oct 31 - Nov 4, 2021. Virtual Conference

EEG Electrode Selection for a Two-Class Motor Imagery Task in a BCI Using fNIRS Prior Data

Amir H. Moslehi, *Student Member, IEEE*, T. Claire Davies, *Member, IEEE*

***Abstract*— This study investigated the possibility of using functional near infrared spectroscopy (fNIRS) during right- and left-hand motor imagery tasks to select an optimum set of electroencephalography (EEG) electrodes for a brain computer interface. fNIRS has better spatial resolution allowing areas of brain activity to more readily be identified. The ReliefF algorithm was used to identify the most reliable fNIRS channels. Then, EEG electrodes adjacent to those channels were selected for classification. This study used three different classifiers of linear and quadratic discriminant analyses, and support vector machine to examine the proposed method.**

***Clinical Relevance*— Reducing the number of sensors in a BCI makes the system more usable for patients with severe disabilities.**

I. Introduction

Electroencephalography (EEG) is the most frequently used imaging technique in brain computer interfaces (BCIs). It is a non-invasive technique that offers high temporal resolution, low cost, and portability. A drawback of EEG is its relatively poor spatial resolution compared to functional magnetic resonance imaging (fMRI) and functional near infrared spectroscopy (fNIRS) [1]. The brain's electrical activities are produced by voltage change across the neurons' cell membranes. The electrical activity generated by a single neuron is too small to be detected by EEG electrodes. Therefore, each EEG electrode records electrical activities due to many neurons in the brain. Each EEG signal consists of a combination of signals originating from different areas of the brain [2]. When attempting to detect EEG signals, the skull and the scalp attenuate the electrical signals produced by the brain's neuronal activities making it more difficult for an EEG system to identify the electrical current source in the brain [3].

The fNIRS is another non-invasive imaging approach that measures the concentration changes of oxy- (HbO) and deoxy-hemoglobin (HbR) molecules in the superficial layer of brain's cortex. These changes occur due to the brain's neuronal activities that also produce the EEG signals. Like EEG, it is portable and low cost compared to fMRI and magnetoencephalography (MEG) and is a suitable option for use outside the laboratory. Furthermore, it offers good spatial resolution, and is less sensitive to electrooculography (EOG) and electromyography (EMG) artifacts compared to EEG [4]. By monitoring the blood flow changes in the brain cortex, the fNIRS systems can detect areas of the brain that are active or nonactive during different tasks. A drawback of the fNIRS is its inherent delay due to slower hemodynamic response compared to the brain's electrical activities. Therefore, using an fNIRS-based BCI in real time may pose challenges due to fNIRS slower response to the brain's neural activities.

Research has shown that standard EEG electrode placement on commercial systems may not target the areas of highest activity in children with cerebral palsy [5]. The main aim of this study was to investigate the use of fNIRS signals to detect active brain areas during motor imagery tasks, and to use this information to select an optimum set of EEG electrodes for classification. Minimizing the number of sensors in a BCI reduces the computational complexity and the set-up time. By combining the advantages of both EEG and fNIRS systems (i.e., fNIRS spatial resolution and EEG's high temporal resolution), this study leads to patient specific BCIs.

II. Methodology

In this study, we used an open-access dataset provided by Shin et al. [6]. A summary of the data is described in sections A, B, and C, while sections D and E describe the analyses.

A. Participants

The data were collected from 29 healthy individuals who reported no neurological or brain-related diseases. The participants consisted of 14 males and 15 females with an average age of 28.5 ± 3.7 years (mean ± standard deviation).

B. Data Acquisition

The EEG data were recorded at 1000 Hz using 30 active electrodes by BrainAmp EEG system (Brain Products GmbH, Gilching, Germany). The linked mastoid was used as reference. The electrodes were placed on a fabric cap (EASYCAP GmbH, Herrsching am Ammersee, Germany) according to the international 10-5 system. An additional electrode was placed at Fz as ground.

The fNIRS data were recorded at 12.5 Hz by NIRScout (NIRx GmbH, Berlin, Germany). A total of 14 transmitters and 16 detectors were placed over the entire head resulting in 36 fNIRS channels. The frontal, motor, and occipital regions consisted of 9, 24, and 3 channels, respectively. The inter-optode distance was kept at 3 cm. Fig.1 illustrates the locations of the EEG and fNIRS sensors in this dataset. The EEG and fNIRS data were down-sampled to 200 and 10 Hz, respectively, by Shin et al. [6].

C. Experimental Paradigm

Each participant performed three sessions of left- and right-hand motor imagery. Fig. 2 depicts the paradigm for each session. As shown, each session begins by 1 minute of rest, followed by 20 repetitions of the task, and ends with 1 minute of rest. The task period started with 2 seconds of visual

* This work was supported by a Discovery Grant from the Natural Science and Engineering Research Council of Canada [NSERC RGPIN 2016-04669].

A. H. Moslehi and T. C. Davies are with the Department of Mechanical and Materials Engineering at Queen's University, Kingston, ON, Canada (e-mail: amir.moslehi@queensu.ca).

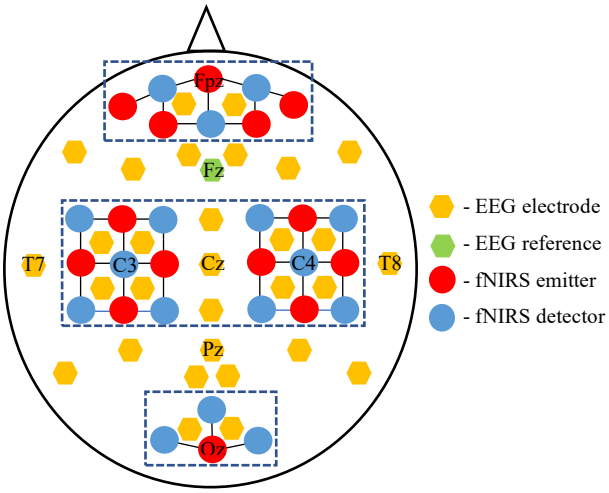

Figure 1. EEG electrodes and fNIRS optodes locations. The EEG electrodes are shown by yellow hexagons. The fNIRS emitters and detectors are shown by red and blue circles, respectively. Each line connecting the circles forms a channel. The frontal, motor, and occipital regions for the fNIRS channels are separated by dashed rectangles.

instructions indicating the hand with which the motor imagery task was to be performed. Following the instructions, the participants performed the task by imagining opening and closing their hands as if they were grabbing a ball at a rate of 1 Hz. Each task period ended by a short rest period which was randomized to be between 15 and 17 seconds. Each hand motor imagery task was done 10 times in each session (30 in total for all three sessions).

D. Data Processing

1) Pre-Processing

The EEG data were pre-processed using the EEGLAB toolbox in MATLAB R2021a (MathWorks in Natick, MA, USA) [7]. First, the raw EEG data were bandpass filtered from 0.5 to 50 Hz with a FIR filter. Then, an automatic artifact rejection tool based on independent component analysis was used to remove artifacts from the EEG signals [8]. Finally, the data were filtered using a 2nd order Butterworth bandpass filter from 8 to 30 Hz to only include signals containing the μ and β frequency bands [9].

The raw fNIRS data were converted to data that represented concentration changes of HbO and HbR according to the modified Beer-Lambert law [10] by the SPM-fNIRS toolbox [11] in MATLAB. The HbO and HbR data were bandpass filtered from 0.01 to 0.2 Hz using a 4th order recursive Butterworth filter to remove artifacts associated with cardiac and respiration noise, and the slow physiological drift in signal [12-14]. Baseline correction was achieved by averaging the data between -5 and 0 s, and then, subtracting the average value from the corresponding task data [15].

2) Feature Extraction

For EEG signals, the event related synchronization (ERS) and desynchronization (ERD) measures were obtained by calculating the relative changes in power during the motor imagery task compared to baseline (rest), and are shown in (1) [16]:

$$ERD/ERS = \frac{P_{task} - P_{Baseline}}{P_{Baseline}} \quad (1)$$

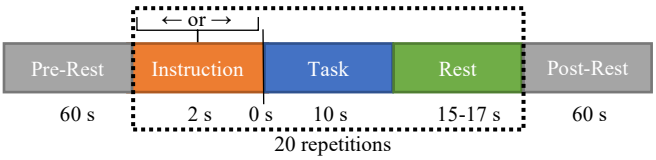

Figure 2. Experimental paradigm.

where P_{task} is the average power over one second during the task, and $P_{Baseline}$ is the average power over one second prior to the task onset.

For fNIRS, the features were calculated by obtaining the mean of HbO (mHbO) over a window of one second during the task according to (2):

$$\mu_w = \frac{1}{N_w}\sum_{k=k_1}^{k_2} \Delta HbO(k) \quad (2)$$

where w denotes window size (i.e., one second), μ_w is the mean for the given window, k_1 and k_2 are the start and end of the window, N_w is the number of observations in the window and is equal to 10 (i.e., 10 Hz × 1 s), and ΔHbO is the HbO data within that window.

3) Channel Selection

This study used the ReliefF algorithm, a filter-based channel selection method, to identify the most relevant fNIRS channels. This algorithm is a computationally efficient channel selection technique that uses the k nearest neighbours approach to assign a weight to each channel [17, 18]. It selects a random instance (xi) and searches its k nearest neighbours and records the number of its neighbours that belong to the same class (hit) and the number of neighbours that belong to a different class (miss). Based on the number of hits and misses, a weight is assigned to each channel. Channels are ranked based on their corresponding weights; those with the highest weights being the most relevant for classification. In this study, a k value of 10 was selected [19, 20].

Two different methods were evaluated using the ReliefF algorithm. First, the top five fNIRS channels with the highest weights of all 36 channels were identified. Second, the top three channels from each brain area were calculated: the frontal, and each hemisphere of the motor cortices. Three motor channels from each hemisphere were selected due to the bilateral hand movement imagery tasks which would result in neural activities in the motor cortex of the contralateral hemisphere [21].

To minimize the number of EEG electrodes, those adjacent to the top five fNIRS channels selected previously were identified. The resulting electrodes were named "Top 5". Similarly, the EEG electrodes adjacent to the top three frontal and top six motor cortex channels were identified. These electrodes were named "F-3" and "M-6", respectively.

4) Classification

Three different supervised machine learning algorithms of linear discriminant analysis (LDA), quadratic discriminant analysis (QDA), and support vector machine (SVM) with quadratic kernel function were used in this study. To evaluate the classification accuracies, a 10-fold cross validation was used for each classifier.

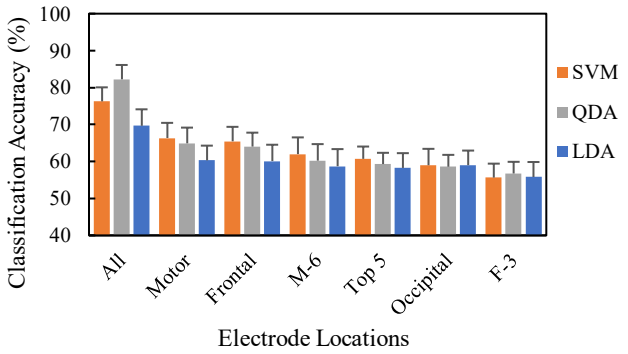

Figure 3. Average classification accuracies for different electrode locations and classifiers.

E. Data Analysis

All statistical analyses were done in IBM SPSS Statistics Ver. 27 (IBM Corp. in Armonk, NY, USA). To examine differences in classification accuracies among electrode selections and classifiers, a two-way (factors: electrode locations and classifiers) repeated measures ANOVA was used to test for significant main effects and interactions. The significance level (alpha) was set at 5%, and Bonferroni correction was used prior to pairwise comparison. In the case of significant interaction effects, simple effects were analyzed by running one-way repeated measures ANOVA twice: once with electrodes selection as factor, and a second time with classifier as factor.

III. Results

Figure 3 and Table 1 depict the average classification accuracies across all participants for different electrode selections (i.e., all, motor, frontal, M-6, Top 5, occipital, and F-3), and classifiers (SVM, QDA, and LDA). As shown, the highest accuracy is obtained when using all electrodes for classification, followed by the electrodes over the motor and frontal cortices.

The statistical analysis revealed significant main effects for both electrode selections ($p < 0.001$) and classifier ($p < 0.001$), and significant interaction effect ($p < 0.001$). Pairwise comparison of the electrode locations showed that using all and the F-3 electrodes resulted in the highest and lowest classification accuracies, respectively, compared to other electrode locations ($p < 0.05$) (see Figure 4). Secondly, the motor and frontal electrodes led to accuracies that were not significantly different from each other ($p > 0.05$).

The pairwise comparison of the classifiers indicated that both SVM and QDA resulted in accuracies that were not

Table 1. Average classification accuracies (in percent) for different electrode locations and classifiers.

Electrode Locations	Classifier		
	SVM	QDA	LDA
All	76.3±3.8	82.2±3.9	69.7±4.5
Motor	66.3±4.1	64.9±4.3	60.3±4.0
Frontal	65.5±3.9	64.0±3.8	60.1±4.4
M-6	62.0±4.5	60.2±4.5	58.7±4.6
Top 5	60.7±3.3	59.3±3.1	58.3±4.0
Occipital	59.0±4.4	58.6±3.2	59.0±3.9
F-3	55.6±3.8	56.7±3.2	55.8±4.1

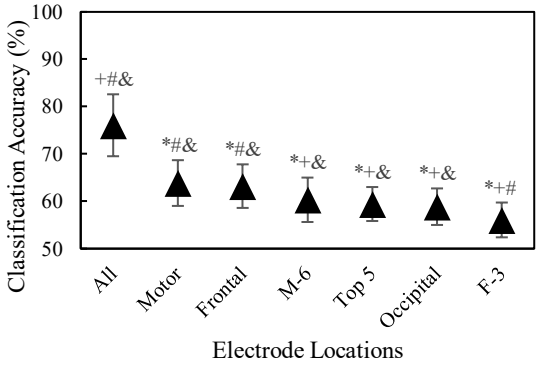

* indicates significant difference from "All" ($p < 0.05$).
\+ indicates significant difference from "Motor" and "Frontal" ($p < 0.05$).
\# indicates significant difference from "M-6", "Top 5", and "Occipital" ($p < 0.05$).
& indicates significant difference from "F-3" ($p < 0.05$).

Figure 4. Average classification accuracies of all classifiers for different electrode locations. Standard deviation is shown by the error bars.

significantly different from each other ($p > 0.05$), and they were both higher than LDA ($p < 0.05$) (see Figure 5).

IV. Discussion

BCIs are technologies that have the potential to help individuals with severe disability interact with their environment using their thoughts rather than their muscles. However, electrode placement may vary as compared to a population without disability. To make the BCIs more usable for the patients outside the laboratory, the number of sensors should be minimized and located effectively. This also reduces the computational complexity of the BCI by removing the redundant or irrelevant sensors from the system.

The ReliefF algorithm used in this study is a filtering channel selection algorithm which has been used in the literature for channel and feature selection and achieved good results. The filtering methods examine the intrinsic properties of the channels and rank them based on their level of importance [22]. For instance, a study used this technique to reduce the number of EEG electrodes from 118 to only 10

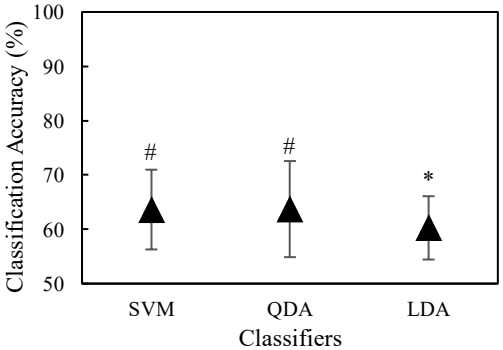

* indicates significant difference from "SVM" and "QDA" ($p < 0.05$).
\# indicates significant difference from "LDA" ($p < 0.05$).

Figure 3. Average classification accuracies of all electrode locations (All, Motor, Frontal, M-6, Top 5, Occipital, and F-3) for different classifiers. Standard deviation is shown by the error bars.

during right hand and right foot motor imagery tasks, and achieved classification accuracies of over 88% [19]. Another study used this algorithm to reduce the number of fNIRS features from 180 to only 5 features for a right- and left-hand motor imagery tasks, and achieved classification accuracies of about 65% [23]. This was higher than when all 180 features were used for classification.

Due to the higher spatial resolution of fNIRS, the channel selection algorithm was applied to identify the highest ranked fNIRS channels over the entire head (Top 5), and the frontal (F-3) and motor (M-6) cortices. Next, the EEG electrodes adjacent to the highest ranked fNIRS channels were identified and used for classification to ensure placement over the areas of highest brain activity. The proposed method in this study resulted in average accuracies of 56.1, 60.3, and 59.4% for F-3, M-6, and Top 5 electrodes, respectively. While these accuracies are significantly lower than when all electrodes were used for classification, the difference in accuracy between all the motor cortex electrodes and the M-6 electrodes was less than 2% for LDA. This difference was larger for SVM and QDA, and was less than 5%. These results can potentially be improved using different algorithms. For instance, Morioka et al. showed the merit of the proposed methodology and estimated the cortical current source during spatial attention tasks by Variational Bayesian Multimodal Encephalography algorithm and the fNIRS signals. Using this method, they were able to classify the EEG signals with an accuracy of close to 80% which was higher than when the fNIRS signals were not used for current source estimation (about 70%) [24].

Future work will involve investigating other channel selection techniques to improve the classification accuracies while minimizing the number of the sensors. For instance, one study used source localization technique to identify the active areas of the brain during motor imagery tasks. Using this method, they reduced the number of EEG electrodes from 64 to only 3, and achieved an accuracy of 74.7% [25]. Different EEG feature extraction technique should be assessed as well, since different techniques result in different accuracies [26].

V. Conclusion

This study proposed a method to identify the location of the brain in which the highest activity occurred using fNIRS to target EEG electrode placement. While this technique provided some insight, more research is needed to improve the localization accuracy using the proposed method.

References

[1] L. F. Nicolas-Alonso and J. Gomez-Gil, "Brain computer interfaces, a review," *Sensors (Basel),* vol. 12, no. 2, pp. 1211-79, 2012.

[2] C. H. Wolters, A. Anwander, X. Tricoche, D. Weinstein, M. A. Koch, and R. S. MacLeod, "Influence of tissue conductivity anisotropy on EEG/MEG field and return current computation in a realistic head model: a simulation and visualization study using high-resolution finite element modeling," *Neuroimage,* vol. 30, no. 3, pp. 813-26, Apr 15 2006.

[3] M. Akhtari *et al.*, "Conductivities of three-layer live human skull," *Brain Topogr,* vol. 14, no. 3, pp. 151-67, Spring 2002.

[4] G. Derosiere, K. Mandrick, G. Dray, T. E. Ward, and S. Perrey, "NIRS-measured prefrontal cortex activity in neuroergonomics: strengths and weaknesses," (in eng), *Front Hum Neurosci,* vol. 7, p. 583, 2013.

[5] S. Taherian, D. Selitskiy, J. Pau, and T. Claire Davies, "Are we there yet? Evaluating commercial grade brain-computer interface for control of computer applications by individuals with cerebral palsy," *Disabil Rehabil Assist Technol,* vol. 12, no. 2, pp. 165-174, Feb 2017.

[6] J. Shin *et al.*, "Open Access Dataset for EEG+NIRS Single-Trial Classification," *IEEE transactions on neural systems and rehabilitation engineering : a publication of the IEEE Engineering in Medicine and Biology Society,* vol. 25, no. 10, pp. 1735-1745, Oct 2017.

[7] A. Delorme and S. Makeig, "EEGLAB: an open source toolbox for analysis of single-trial EEG dynamics including independent component analysis,", *Journal of neuroscience methods,* vol. 134, no. 1, pp. 9-21, Mar 15 2004.

[8] I. Winkler, S. Haufe, and M. Tangermann, "Automatic classification of artifactual ICA-components for artifact removal in EEG signals," *Behav Brain Funct,* vol. 7, no. 1, p. 30, Aug 2 2011.

[9] A. M. Chiarelli, P. Croce, A. Merla, and F. Zappasodi, "Deep learning for hybrid EEG-fNIRS brain-computer interface: application to motor imagery classification," *J Neural Eng,*vol. 15, no. 3, p. 036028, Jun 2018.

[10] D. T. Delpy, M. Cope, P. van der Zee, S. Arridge, S. Wray, and J. Wyatt, "Estimation of optical pathlength through tissue from direct time of flight measurement," *Phys Med Biol,* vol. 33, no. 12, pp. 1433-42, Dec 1988.

[11] S. Tak, M. Uga, G. Flandin, I. Dan, and W. D. Penny, "Sensor space group analysis for fNIRS data," (in eng), *Journal of neuroscience methods,* vol. 264, pp. 103-112, May 1 2016.

[12] A. H. Moslehi, M. Bagheri, A. Ludwig, and T. C. Davies, "Discrimination of Two-Class Motor Imagery in a fNIRS Based Brain Computer Interface," in *2020 42nd Annual International Conference of the IEEE Engineering in Medicine & Biology Society (EMBC)*, 20-24 July 2020 2020, pp. 4051-4054.

[13] A. P. Buccino, H. O. Keles, and A. Omurtag, "Hybrid EEG-fNIRS Asynchronous Brain-Computer Interface for Multiple Motor Tasks," *PLoS One,* vol. 11, no. 1, p. e0146610, 2016.

[14] R. Li, T. Potter, W. Huang, and Y. Zhang, "Enhancing Performance of a Hybrid EEG-fNIRS System Using Channel Selection and Early Temporal Features," (in eng), *Front Hum Neurosci,* vol. 11, p. 462, 2017.

[15] S. C. Wriessnegger, G. Bauernfeind, E. M. Kurz, P. Raggam, and G. R. Muller-Putz, "Imagine squeezing a cactus: Cortical activation during affective motor imagery measured by functional near-infrared spectroscopy," (in eng), *Brain Cogn,* vol. 126, pp. 13-22, Oct 2018.

[16] G. Pfurtscheller, "Functional brain imaging based on ERD/ERS," *Vision Res,* vol. 41, no. 10-11, pp. 1257-60, 2001/05/01/ 2001.

[17] I. Kononenko, "Estimating attributes: Analysis and extensions of RELIEF," Berlin, Heidelberg, 1994: Springer Berlin Heidelberg, in Machine Learning: ECML-94, pp. 171-182.

[18] R. J. Urbanowicz, M. Meeker, W. La Cava, R. S. Olson, and J. H. Moore, "Relief-based feature selection: Introduction and review," *J Biomed Inform,* vol. 85, pp. 189-203, Sep 2018.

[19] A. Franklin Alex Joseph and C. Govindaraju, "Minimizing electrodes for effective brain computer interface," *Biomedical Signal Processing and Control,* vol. 63, p. 102201, 2021/01/01/ 2021.

[20] S. Ge *et al.*, "Neural Activity and Decoding of Action Observation Using Combined EEG and fNIRS Measurement," (in eng), *Front Hum Neurosci,* vol. 13, p. 357, 2019.

[21] R. Beisteiner, P. Hollinger, G. Lindinger, W. Lang, and A. Berthoz, "Mental representations of movements. Brain potentials associated with imagination of hand movements," *Electroencephalogr Clin Neurophysiol,* vol. 96, no. 2, pp. 183-93, Mar 1995.

[22] M. Z. Baig, N. Aslam, and H. P. H. Shum, "Filtering techniques for channel selection in motor imagery EEG applications: a survey," *Artificial Intelligence Review,*vol. 53,no. 2, pp. 1207-1232, 2020/02/01.

[23] E. A. Aydin, "Subject-Specific feature selection for near infrared spectroscopy based brain-computer interfaces," *Comput Methods Programs Biomed,* vol. 195, p. 105535, Oct 2020.

[24] H. Morioka *et al.*, "Decoding spatial attention by using cortical currents estimated from electroencephalography with near-infrared spectroscopy prior information," *Neuroimage,* vol. 90, pp. 128-39, Apr 15 2014.

[25] S. Ge *et al.*, "A Brain-Computer Interface Based on a Few-Channel EEG-fNIRS Bimodal System," *IEEE Access,* vol. 5, pp. 208-218, 2017.

[26] F. Lotte *et al.*, "A review of classification algorithms for EEG-based brain-computer interfaces: a 10 year update," *J Neural Eng,* vol. 15, no. 3, p. 031005, Jun 2018.